Accepted Manuscript

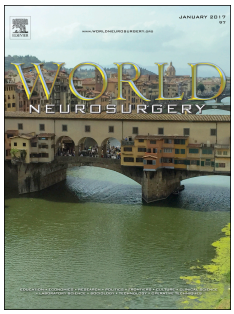

Modular classification of endoscopic endonasal transsphenoidal approaches to the sellar region: anatomical quantitative study

Francesco Belotti, MD, Francesco Doglietto, MD, PhD, Alberto Schreiber, MD, Marco Ravanelli, MD, Marco Ferrari, MD, Davide Lancini, MD, Vittorio Rampinelli, MD, Lena Hirtler, MD, Barbara Buffoli, PhD, Andrea Bolzoni Villaret, MD, Roberto Maroldi, MD, Luigi Fabrizio Rodella, MD, MSc, Piero Nicolai, MD, Marco Maria Fontanella, MD

PII: S1878-8750(17)31681-9

DOI: 10.1016/j.wneu.2017.09.165

Reference: WNEU 6609

To appear in: *World Neurosurgery*

Received Date: 20 July 2017

Revised Date: 22 September 2017

Accepted Date: 23 September 2017

Please cite this article as: Belotti F, Doglietto F, Schreiber A, Ravanelli M, Ferrari M, Lancini D, Rampinelli V, Hirtler L, Buffoli B, Villaret AB, Maroldi R, Rodella LF, Nicolai P, Fontanella MM, Modular classification of endoscopic endonasal transsphenoidal approaches to the sellar region: anatomical quantitative study, *World Neurosurgery* (2017), doi: 10.1016/j.wneu.2017.09.165.

Modular classification of endoscopic endonasal transsphenoidal approaches to the sellar region: anatomical quantitative study

Francesco Belotti, MD,[1*] Francesco Doglietto, MD, PhD,[1*] Alberto Schreiber, MD,[2] Marco Ravanelli, MD,[3] Marco Ferrari, MD,[2] Davide Lancini, MD,[2] Vittorio Rampinelli, MD,[2] Lena Hirtler, MD,[3] Barbara Buffoli, PhD,[4] Andrea Bolzoni Villaret, MD,[2] Roberto Maroldi, MD,[3&] Luigi Fabrizio Rodella, MD, MSc,[4&] Piero Nicolai, MD,[2&] Marco Maria Fontanella, MD[1&]

Units of [1]Neurosurgery, [2]Otorhinolaryngology and [4]Radiology, Department of Medical and Surgical Specialties, Radiological Sciences and Public Health, University of Brescia, Brescia, Italy

[3]Department of Systematic Anatomy, Center for Anatomy and Cell Biology, Medical University of Vienna

[4]Section of Anatomy and Pathophysiology, Department of Clinical and Experimental Sciences, University of Brescia, Brescia, Italy

* These authors equally contributed to the study

[&] These authors equally contributed to the study

Corresponding author

Francesco Doglietto, MD, PhD

Neurosurgery, Department of Medical and Surgical Specialties, Radiological Sciences and Public Health, University of Brescia

Largo Spedali Civili, 1

25123 Brescia, Italy

Phone: +39 030 3995587

Fax: +39 030 3995008

Email: francesco.doglietto@unibs.it

Keywords: Approaches, classification, endoscopy, modular, quantification, transsphenoidal.

Running head: Modular classification of transsphenoidal approaches

Abstract

Background: Endoscopic visualization does not necessarily correspond to an adequate working space. The need of balancing invasiveness and adequacy of sellar tumor exposure has recently led to the description of multiple endoscopic endonasal transsphenoidal approaches. Comparative anatomical data on these variants are lacking.

Object: To quantitatively compare endoscopic endonasal transsphenoidal approaches to the sella and parasellar region, using the concept of "surgical pyramid".

Methods: Four endoscopic transsphenoidal approaches were performed in 10 injected specimens: 1. hemisphenoidotomy; 2. transrostral; 3. extended transrostral (with superior turbinectomy); 4. extended transrostral with posterior ethmoidectomy. ApproachViewer software (part of GTX-Eyes II) with a dedicated navigation system was used to quantify the surgical pyramid volume, as well as exposure of sellar and parasellar areas.. Statistical analyses were performed with Friedman's tests and Nemenyi's procedure.

Results: Hemisphenoidotomy provided limited exposure of the sellar area and a small working volume. A transrostral approach was necessary to expose the entire sella. Exposure of lateral parasellar areas required superior turbinectomy or posterior ethmoidectomy. The differences between each of the modules was statistically significant.

Conclusion: The present study validates, from an anatomical point of view, a modular classification of endoscopic endonasal transsphenoidal approaches to the sellar region.

Abbreviations: 3D: three dimensional; CT: computed tomography; DICOM: Digital Imaging and COmmunications in Medicine; ETA: Extended Transrostral Approach; GTxEyesII – UHN: Guided-Therapeutics software developed at University Health Network – Toronto, Canada; HD: high-definition; HS: Hemisphenoidotomy; PEA: extended transrostral with Posterior Ethmoidectomy Approach; TRA: Transrostral Approach.

Introduction

Endoscopic transnasal surgery provides access to several regions of the skull base, including the sellar region and cavernous sinuses, using the natural corridors constituted by the nasal cavities and sphenoid sinus. Several endoscopic transsphenoidal approaches to the sella and parasellar areas have been recently described,[1-13] but relatively limited clinical, and even anatomical, comparative data are available.

These variations of endoscopic transsphenoidal surgery result from the need of balancing invasiveness with adequacy of sellar tumor exposure. In endoscopic surgery satisfactory visualization is possible even through small openings, which might not grant a reasonable working space; the insufficient opening of the anterior wall of the sphenoid sinus and the sella has been associated with a higher rate of incomplete pituitary adenoma resections.[14,15]

The aim of the present study was to quantify the working volume and exposed areas of different endoscopic transsphenoidal approaches using a novel anatomical research method that quantifies the surgical pyramid, which describes the essential features of a surgical approach.[16,17]

Materials and Methods

Ten human, adult heads were dissected in the Anatomy Laboratory of the University of Brescia: three were fresh frozen and 7 alcohol-fixed. The arterial system was injected via the common carotid and vertebral arteries with silicone rubber (Xiameter® RTV rubber base and curing agent, Dow Corning, Midland, MI, USA) stained with red Pintasol (Mixol® Red E-L3mix, Kirchheim unter Teck, Germany).

The specimens underwent computed tomography (CT) scan using a multidetector 128-slice scanner (Somatom Definition Flash®, Siemens, Forcheim, Germany) set with standard neuronavigation parameters. The CT scan files were recorded in Digital Imaging and COmmunications in Medicine (DICOM) format.

Two fresh specimens were dissected at the Anatomy Laboratory of the University of Vienna. Arterial injections were performed with the same method as above. The fresh specimens were not included in the statistical analysis but used only to collect video material.

All specimens had a sellar type sphenoid sinus.[18,19]

Transsphenoidal approaches

Dissections at the University of Brescia were performed using a high-definition (HD) head-camera with 0° endoscope (Karl Storz®, Tuttlingen, Germany) and an endoscopic pituitary and skull base surgery set (Karl Storz®). Four increasingly extended endoscopic endonasal transsphenoidal approaches were performed bilaterally. The approaches based on the transsphenoidal corridor, as

defined in the classification by the Cornell group,[20] were considered for the study, except for the transplanum/transtuberculum approach, because our study was focused on lateral extension. Furthermore, the four approaches considered in this study correspond to the steps described by the Pittsburgh group to perform the endoscopic approach to the sella turcica, the parasellar structures, and the middle third of the clivus,[21,22] with the addition of the posterior ethmoidectomy. Each approach was quantified before performing the subsequent one. The posterior wall and floor of the sphenoid sinuses were left intact throughout the dissections.

Hemisphenoidotomy (HS)[8,12,13] began with lateralization of the middle and superior turbinates. The sphenoid ostium was enlarged from the sphenoid rostrum to the superior turbinate, from the planum ethmoidalis to the floor of the sphenoid sinus.[23] Sinus mucosa and sphenoid septa were removed to better visualize anatomic landmarks inside the sphenoid sinus (Figure 1 and video 1).

The *Transrostral Approach* (TRA) was performed via binostril dissection,[3,23] after completing the HS bilaterally. The posterior portion of the septum was disarticulated from the sphenoid rostrum. Next, a posterior septectomy,[1,24] which needs to be about 1 cm wide to allow binostril access,[1,2] was performed. Subsequently, the sphenoid sinus anterior wall was removed, exposing the posterior wall from carotid prominence to carotid prominence, and from the planum to the clivus craniocaudally.[3] Special attention was given to widening the sphenoidectomy as much as possible: the initial rhomboid shape after rostrum removal was thus transformed in a rectangular shaped opening (Figure 2 and video 2).

The *Extended Transrostral Approach* (ETA) was performed by adding a superior turbinectomy to TRA.[25] The superior turbinate was transected close to the skull base.[24,26] The sphenoidotomy was then extended supero-laterally until the medial wall of the posterior ethmoid was reached (Figure 3 and video 3).

The *Extended Transrostral with Posterior Ethmoidectomy Approach* (PEA) was accomplished by removing the posterior ethmoid cells,[25-29] which were opened in a posterior-to-anterior direction.[30] The resection was carried on until the basal lamella was reached.[30] Next, the previous opening of the anterior sphenoid sinus wall was extended to the posterior wall of the ethmoid sinuses (Figure 4 and video 4).

Dissections at the University of Vienna were performed using a 3D-HD 0° endoscope (VSiii, VisionSense, Petach Tikva, Israel) and an endoscopic pituitary and skull base surgery set (Karl Storz®) (videos 1-4).

Quantitative analysis

Quantitative comparison of approaches was based on anatomical features, defining them as “truncated pyramids” according to Andaluz et al.[16,17] The surgical pyramid is defined by: superficial surface

(surgical window); deep surface (area of exposure); height (the distance between those areas); and pyramid volume (space available for instruments). In transsphenoidal endoscopy, the superficial surface is the nostril at the level of the pyriform aperture. The deep surface is the posterior wall of the sphenoid sinus. Superficial area and height are common features among transsphenoidal approaches. Therefore, volumes and deep areas were the object of the present study.

ApproachViewer, which is the software incorporated in GTxEyesII – UHN, a neuronavigation system that has been developed at the University of Toronto, was used for quantification.[31] The navigation hardware was by NDI (Northern Digital Imaging®, Waterloo, Ontario, Canada) and included a passive rigid body, passive probe (pointer) with 4 markers, and the Polaris Vicra® Optical Tracking System. The Polaris optical camera emits infrared (IR) light and captures the IR reflections off sphere markers attached to the pointer, whose geometry allows reproducing its position and orientation via multiplanar reconstruction. DICOM files were uploaded in GTxEyesII software and registration tolerance of less than 1 mm was considered acceptable.

In addition to standard neuronavigation, this software allows the collection of deep and superficial surfaces using the pointer to track their perimeters, thus providing real-time visualization and quantification of the surgical pyramid in axial, coronal, and sagittal sections, as a 3D rendering (Figure 5). The quantification procedure was repeated twice for each approach, tracking both “non-crossing” and “crossing” pyramids (Figure 6). A non-crossing pyramid is realized by keeping the pointer in corresponding positions on the deep and the superficial surfaces (i.e. 3 o’clock at both the pyriform aperture and posterior wall of the sphenoid sinus), while tracing the deep surface perimeter, obtaining the obstacle-free working space granted by the approach. In contrast, a crossing pyramid is obtained by keeping the pointer in opposite position on deep and superficial surfaces (i.e. 3 o’clock at the pyriform aperture and 9 o’clock at the posterior wall of the sphenoid sinus), defining the maximum reachable deep surface.

ApproachViewer allows also post-dissection analyses by drawing any areas of interest on CT scans. Contouring is performed by tracing the desired surface in each consecutive axial CT slice to generate the surface. ApproachViewer then matches each surgical pyramid with each area of interest, providing the absolute and percentage values of target surfaces exposed by each.

The 14 contoured surfaces, located below the tuberculum sellae and above the sphenoid floor, are shown in figure 7 (see figure for further details).

Each surface was quantified from both nostrils (ipsilateral and contralateral).

Statistical analysis

Statistical analyses were performed with non-parametric analysis of variance Friedman’s tests using XL-STAT® statistical software (Addinsoft, Paris, France) to compare each approach for volume and

exposed areas. The tests were performed on 20 sides, except for areas that were not present in all specimens due to anatomical variations, i.e. clival recess, 16 sides, and VR-line surfaces, 19 sides. Subsequently, post-hoc tests using the Nemenyi's procedure were performed to obtain pairwise comparisons. A p-value < 0.05 was considered statistically significant for both Friedman's and post-hoc tests.

Results

The statistical analysis of surgical volumes (Figure 5) showed that ETA and PEA had larger volumes than HS and TRA ($p < 0.05$). In addition, TRA had a significantly larger volume than HS ($p < 0.05$).

The values of mean percentage value of exposed area by non-crossing and crossing surgical volumes are shown in the radar charts of Figure 8. All Friedman's tests showed positive results ($p < 0.05$). Significant pairwise comparisons are reported as a graphical representation in Figure 9.

Analyzing the results regarding the ipsilateral Sella – half, the non-crossing HS was proven to cover a significantly smaller surface compared to the other approaches except for the crossing HS and the non-crossing TRA. Furthermore, the crossing HS was significantly smaller than crossing and non-crossing PEA.

The results regarding the contralateral Sella – half showed that the non-crossing HS was smaller than all the other approaches except for the crossing HS. Moreover, the percentage of surface covered performing the crossing HS was significantly lower than all the other crossing approaches.

The results regarding the ipsilateral ICA – medial half showed that non-crossing HS and TRA covered less surface than crossing and non-crossing PEA.

The contralateral ICA – medial half was significantly less covered using the non-crossing HS compared to all the other approaches except for the crossing HS and the non-crossing TRA. Non-crossing HS and TRA were smaller than crossing approaches subsequent to their respective ones.

The results regarding the ipsilateral ICA – lateral half showed that non-crossing HS and TRA covered significantly less surface compared to non-crossing and crossing ETA and PEA.

The contralateral ICA – lateral half showed that non-crossing HS and TRA covered significantly less surface than crossing approaches subsequent to their respective ones. On the contrary the non-crossing and the crossing ETA were significantly different. In addition, the crossing HS was significantly smaller than crossing TRA, ETA and PEA.

The inter-ICA distance proved that there was a difference between the non-crossing HS and all the other approaches, except for the crossing HS; which was significantly smaller compared to crossing and non-crossing TRA, ETA, and PEA.

The clival recess showed that the non-crossing HS was significantly smaller than crossing TRA, ETA, and PEA; and the non-crossing ETA and PEA.

The results regarding ipsilateral and contralateral paraclival ICAs showed that the non-crossing HS and TRA covered significantly less surface compared to all crossing approaches, except for their respective ones. Moreover, only for the contralateral surface, crossing ETA and PEA were larger than their non-crossing respective approaches. Instead, only for the ipsilateral surface, non-crossing ETA and PEA were bigger than the non-crossing HS; and non-crossing PEA was also larger than non-crossing TRA. The crossing HS was smaller than crossing ETA, PEA and TRA (only for the contralateral surface).

The results regarding the ipsilateral Gasserian ganglion showed that the non-crossing HS and the non-crossing TRA covered less surface compared crossing ETA and PEA. The crossing HS was smaller than the crossing ETA and PEA.

The contralateral Gasserian ganglion showed that the crossing ETA and PEA covered more surface than non-crossing HS, TRA, and ETA; and the crossing HS. In addition, the crossing PEA was also superior to crossing TRA and non-crossing PEA.

The results regarding the ipsilateral VR-line surface showed that non-crossing HS and TRA were significantly smaller than the crossing PEA. The contralateral VR-line surface showed that the crossing PEA covered more surface than all non-crossing approaches and the crossing HS.

Discussion

There is disagreement on advantages and limitations of endoscopic transsphenoidal approaches for the treatment of sellar tumors with variable nasal invasiveness.[32-34] Insufficient opening of the sphenoid sinus is a relatively common error in transsphenoidal surgery (ETS)[3,14,15] and has been related to an increased risk for pituitary adenoma remnant or recurrence.[14,15] On the other hand, increased invasiveness of the approach can lead to sinonasal morbidity.[35,36]

The aim of the present study was to contribute to this debate by quantifying working volume and exposure of four endoscopic transsphenoidal approaches with increasing nasal invasiveness.

ApproachViewer allowed for quantitative comparison of the approaches based on their anatomical features, i.e. “truncated pyramids”.[17] The quantification process was performed with two different modalities. The aim of non-crossing quantifications was to define the largest “working” volume, i.e. the volume, free of obstacles, that has the highest surgical maneuverability for bimanual surgery, as each point of the exposed area can be reached by two straight instruments entering from any point of the superficial area. The crossing quantifications documented the widest area of exposure, reached by a straight instrument.

The results of this study showed that HS provides a limited working volume, characterized by a long and narrow tunnel, which explains the limited variability between non-crossing and crossing volumes. In HS, the sphenoid rostrum limits exposure of the sphenoid contralateral to the nostril used for the

approach. The role of HS has indeed been limited to small lateral pituitary lesions of soft consistency.[8,12,13] Some authors[4,5,7,8,37,38] extended the clinical applications of HS by adding removal of the rostrum and therefore performing a TRA, which allows a significantly larger working volume, sphenoidotomy and exposure, as documented herein. TRA was the less invasive approach that exposes the sella. While ispilateral areas were not significantly more exposed, contralateral ones were, as previously reported by others in clinical practice.[4,5,37] A binostril technique would intuitively allow a sum of the working volumes, increasing the maneuverability of instruments.[1,3] Recently a variation of TRA, which entails a submucosal dissection on one side (video 1), has been described to allow a binostril approach, but at the same time possibly diminishing nasal morbidity.[10]

Increased exposure of the ipsilateral parasellar region was achieved with ETA and PEA. Although some authors have described ETA and PEA,[24,26,29] a precise indication is still lacking. Superior turbinectomy was not always performed before posterior ethmoidectomy.[39,40] Anatomically, this study showed that ETA and PEA should be performed as modular approaches, which provide increasing working volume and exposure of the parasellar area.

Possible future implications of this study include optimization of surgical instruments for ETS. Non-crossing volumes provide a detailed description of the working space, while crossing volumes provide the maximal exposure obtained with straight instruments. As the endoscope provides a wide, panoramic view, even through small openings, the surgeon can compensate the restricted working volume with angled instruments that might allow reaching areas that are outside those reached by the crossing modality. Nonetheless, these instruments must go through the non-crossing volume: if this is too small, then flexible instrumentation that can be bent at the level of the sphenoid (i.e. past the restriction of the endonasal corridor) might represent a solution.

Limitations of the present study

This is an anatomical quantitative study, which was limited to the median variations of endoscopic transsphenoidal approaches to the sellar region. A quantification of the reported approaches in the clinical setting is also required to validate this modular classification. Furthermore, prospective analysis of clinical outcomes, with comparative data, will be needed and is on-going in our centre. Nonetheless, this study follows the IDEAL recommendations,[41] fully exploiting the preclinical phase of surgical research.

Conclusions

HS, TRA, ETA, and PEA approaches constitute a modular classification of endoscopic transsphenoidal surgery for sellar lesions, with increasing nasal invasiveness, working volume, and exposure of the parasellar region.

The results of this anatomical study correlate well with the intuitions gained from clinical practice, adding weight to the potential of pre-clinical, anatomical research in surgery. In addition, the data collected might also be useful towards the efficient design of new surgical instruments, especially if curved or flexible.

Acknowledgements

We thank Prof. Rita Rezzani, Head of the Section of Anatomy and Pathophysiology, University of Brescia, for study supervision and Marco Angelo Cocchi, MSc (Section of Anatomy and Pathophysiology, University of Brescia) for the support during the dissection sessions.

Disclosure

The authors report no conflict of interest concerning the materials or methods used in this study or the findings specified in this paper.

References

1. P. Cappabianca, L. Cavallo, I. Esposito, M. Tschabitscher. Transsphenoidal Approaches: Endoscopic. In: P Cappabianca, G Iaconetta, L Califano, eds. *Cranial, Craniofacial and Skull Base Surgery*: Springer Milan; 2010:197-212.
2. P. Cappabianca, L. M. Cavallo, F. Esposito, V. Stagno, M. G. De Notaris. 12 - Endoscopic Transsphenoidal Surgery: Anatomy, Instrumentation, Techniques. In: ERL Lanzino, ed. *Transsphenoidal Surgery*. Saint Louis: W.B. Saunders; 2010:128-142.
3. A. R. Dehdashti, A. Ganna, K. Karabatsou, F. Gentili. Pure endoscopic endonasal approach for pituitary adenomas: early surgical results in 200 patients and comparison with previous microsurgical series. *Neurosurgery*. 2008;62(5):1006-1015; discussion 1015-1007.
4. M. Berhouma, M. Messerer, E. Jouanneau. Occam's razor in minimally invasive pituitary surgery: tailoring the endoscopic endonasal uninostril trans-sphenoidal approach to sella turcica. *Acta neurochirurgica.* 2012;154(12):2257-2265.
5. H. D. Jho. Endoscopic pituitary surgery. *Pituitary.* 1999;2(2):139-154.
6. H. D. Jho, R. L. Carrau. Endoscopic endonasal transsphenoidal surgery: experience with 50 patients. *Journal of neurosurgery.* 1997;87(1):44-51.
7. S. Linsler, M. R. Gaab, J. Oertel. Endoscopic endonasal transsphenoidal approach to sellar lesions: a detailed account of our mononostril technique. *Journal of neurological surgery Part B, Skull base.* 2013;74(3):146-154.
8. L. Tataranu, M. Gorgan, V. Ciubotaru. Endoscopic endonasal transsphenoidal approach in the management of sellar and parasellar lesions: alternative surgical techniques, results, complications (Part II). *Romanian Neurosurgery.* 2010;17:182-191.
9. M. Kutlay, E. Gonul, B. Duz, Y. Izci, O. Tehli, C. Temiz, et al. The use of a simple self-retaining retractor in the endoscopic endonasal transsphenoidal approach to the pituitary macroadenomas: technical note. *Neurosurgery.* 2013;73(2 Suppl Operative):ons206-209; discussion ons209-210.
10. S. Nie, K. Li, Y. Huang, J. Zhao, X. Gao, J. Sun. Endoscopic endonasal transsphenoidal surgery for treating pituitary adenoma via a sub-septum mucosa approach. *International Journal of Clinical and Experimental Medicine.* 2015;8(4):5137-5143.
11. V. Waran, I. P. Tang, R. Karuppiah, K. A. Abd Kadir, H. Chandran, K. A. Muthusamy, et al. A new modified speculum guided single nostril technique for endoscopic transnasal transsphenoidal surgery: an analysis of nasal complications. *Br J Neurosurg.* 2013;27(6):742-746.

12. E. de Divitiis, P. Cappabianca, L. M. Cavallo. Endoscopic transsphenoidal approach: adaptability of the procedure to different sellar lesions. *Neurosurgery.* 2002;51(3):699-705; discussion 705-697.
13. D. B. Moreland, E. Diaz-Ordaz, G. A. Czajka. Endoscopic endonasal hemisphenoidotomy for resection of pituitary lesions confined to the sella: report of 3 cases and technical note. *Minim Invasive Neurosurg.* 2000;43(2):57-61.
14. H. Alahmadi, A. R. Dehdashti, F. Gentili. Endoscopic endonasal surgery in recurrent and residual pituitary adenomas after microscopic resection. *World neurosurgery.* 2012;77(3-4):540-547.
15. C. A. Mattozo, J. R. Dusick, F. Esposito, H. Mora, P. Cohan, D. Malkasian, et al. Suboptimal sphenoid and sellar exposure: a consistent finding in patients treated with repeat transsphenoidal surgery for residual endocrine-inactive macroadenomas. *Neurosurgery.* 2006;58(5):857-865; discussion 857-865.
16. F. Doglietto, I. Radovanovic, M. Ravichandiran, A. Agur, G. Zadeh, J. Qiu, et al. Quantification and comparison of neurosurgical approaches in the preclinical setting: literature review. *Neurosurg Rev.* 2016;39(3):357-368.
17. N. Andaluz, H. R. Van Loveren, J. T. Keller, M. Zuccarello. Anatomic and clinical study of the orbitopterional approach to anterior communicating artery aneurysms: in reply. *Neurosurgery.* 2004;54(4):1032.
18. C. A. Hamberger, G. Hammer, G. Norlen, B. Sjogren. Transantrosphenoidal hypophysectomy. *Arch Otolaryngol.* 1961;74:2-8.
19. G. Hammer, C. Radberg. The sphenoidal sinus. An anatomical and roentgenologic study with reference to transsphenoid hypophysectomy. *Acta radiol.* 1961;56:401-422.
20. T. H. Schwartz, J. F. Fraser, S. Brown, A. Tabaee, A. Kacker, V. K. Anand. Endoscopic cranial base surgery: classification of operative approaches. *Neurosurgery.* 2008;62(5):991-1002; discussion 1002-1005.
21. A. Kassam, C. H. Snyderman, A. Mintz, P. Gardner, R. L. Carrau. Expanded endonasal approach: the rostrocaudal axis. Part I. Crista galli to the sella turcica. *Neurosurg Focus.* 2005;19(1):E3.
22. A. Kassam, C. H. Snyderman, A. Mintz, P. Gardner, R. L. Carrau. Expanded endonasal approach: the rostrocaudal axis. Part II. Posterior clinoids to the foramen magnum. *Neurosurg Focus.* 2005;19(1):E4.
23. G. Frank, E. Pasquini, G. Farneti, M. Faustini Fustini. 13 - Endoscopic Transsphenoidal Surgery: Results and Complications. In: ERL Lanzino, ed. *Transsphenoidal Surgery*. Saint Louis: W.B. Saunders; 2010:143-156.

24. G. Har-El, R. M. Swanson. The superior turbinectomy approach to isolated sphenoid sinus disease and to the sella turcica. *Am J Rhinol.* 2001;15(2):149-156.
25. P. Cappabianca, L. M. Cavallo, O. de Divitiis, M. de Angelis, C. Chiaramonte, D. Solari. Endoscopic Endonasal Extended Approaches for the Management of Large Pituitary Adenomas. *Neurosurg Clin N Am.* 2015;26(3):323-331.
26. G. Har-El. Endoscopic transnasal transsphenoidal pituitary surgery--comparison with the traditional sublabial transseptal approach. *Otolaryngol Clin North Am.* 2005;38(4):723-735.
27. D. Simmen, N. Jones. 5 - How? Operative Procedures: A Step-by-Step Safe and Logical Approach. In: D Simmen, N Jones, eds. *Manual of Endoscopic Sinus Surgery and Its Extended Applications*: Thieme; 2005:50-105.
28. A. B. Kassam, D. M. Prevedello, R. L. Carrau, C. H. Snyderman, A. Thomas, P. Gardner, et al. Endoscopic endonasal skull base surgery: analysis of complications in the authors' initial 800 patients. *Journal of neurosurgery.* 2011;114(6):1544-1568.
29. Y. Fujimoto, H. F. Ramos, P. P. Mariani, F. R. Romano, A. Cukiert, E. Bor-Seng-Shu, et al. Superior turbinectomy: role for a two-surgeon technique in endoscopic endonasal transsphenoidal surgery--technical note. *Neurol Med Chir (Tokyo).* 2015;55(4):345-350.
30. B. Abuzayed, N. Tanriover, N. Gazioglu, G. Z. Sanus, F. Ozlen, H. Biceroglu, et al. Endoscopic endonasal anatomy and approaches to the anterior skull base: a neurosurgeon's viewpoint. *J Craniofac Surg.* 2010;21(2):529-537.
31. F. Doglietto, J. Qiu, M. Ravichandiran, I. Radovanovic, F. Belotti, A. Agur, et al. Quantitative comparison of cranial approaches in the anatomy laboratory: A neuronavigation-based research method. *World J Methodol.* 2017;In press.
32. A. N. Mamelak. Pro: endoscopic endonasal transsphenoidal pituitary surgery is superior to microscope-based transsphenoidal surgery. *Endocrine.* 2014;47(2):409-414.
33. P. Mortini. Cons: endoscopic endonasal transsphenoidal pituitary surgery is not superior to microscopic transsphenoidal surgery for pituitary adenomas. *Endocrine.* 2014;47(2):415-420.
34. M. de Notaris, A. Prats-Galino, J. Ensenat, T. Topczewski, E. Ferrer, L. M. Cavallo, et al. Quantitative analysis of progressive removal of nasal structures during endoscopic suprasellar approach. *Laryngoscope.* 2014;124(10):2231-2237.
35. C. F. Thompson, J. D. Suh, Y. Liu, M. Bergsneider, M. B. Wang. Modifications to the Endoscopic Approach for Anterior Skull Base Lesions Improve Postoperative Sinonasal Symptoms. *Journal of neurological surgery Part B, Skull base.* 2014;75(1):65-72.
36. J. R. de Almeida, I. J. Witterick, P. J. Gullane, F. Gentili, L. Lohfeld, J. Ringash, et al. Physical morbidity by surgical approach and tumor location in skull base surgery. *Head & neck.* 2013;35(4):493-499.

37. D. H. Jho, D. H. Jho, H.-D. Jho. Chapter 22 - Endoscopic Endonasal Pituitary and Skull Base Surgery. In: A Quiñones-Hinojosa, ed. *Schmidek and Sweet Operative Neurosurgical Techniques (Sixth Edition)*. Philadelphia: W.B. Saunders; 2012:257-279.
38. R. L. Carrau, A. B. Kassam, C. H. Snyderman. Pituitary surgery. *Otolaryngol Clin North Am.* 2001;34(6):1143-1155, ix.
39. R. R. Orlandi, D. C. Lanza, W. E. Bolger, D. M. Clerico, D. W. Kennedy. The forgotten turbinate: the role of the superior turbinate in endoscopic sinus surgery. *Am J Rhinol.* 1999;13(4):251-259.
40. W. E. Bolger, A. S. Keyes, D. C. Lanza. Use of the superior meatus and superior turbinate in the endoscopic approach to the sphenoid sinus. *Otolaryngol Head Neck Surg.* 1999;120(3):308-313.
41. P. McCulloch, D. G. Altman, W. B. Campbell, D. R. Flum, P. Glasziou, J. C. Marshall, et al. No surgical innovation without evaluation: the IDEAL recommendations. *Lancet.* 2009;374(9695):1105-1112.
42. A. Alfieri, H. D. Jho. Endoscopic endonasal cavernous sinus surgery: an anatomic study. *Neurosurgery.* 2001;48(4):827-836; discussion 836-827.
43. R. Reisch, L. Vutskits, R. Filippi, L. Patonay, G. Fries, A. Perneczky. Topographic microsurgical anatomy of the paraclinoid carotid artery. *Neurosurg Rev.* 2002;25(3):177-183.
44. E. Knosp, E. Steiner, K. Kitz, C. Matula. Pituitary adenomas with invasion of the cavernous sinus space: a magnetic resonance imaging classification compared with surgical findings. *Neurosurgery.* 1993;33(4):610-617; discussion 617-618.
45. J. Wang, S. Bidari, K. Inoue, H. Yang, A. Rhoton, Jr. Extensions of the sphenoid sinus: a new classification. *Neurosurgery.* 2010;66(4):797-816.
46. T. H. Elkammash, M. M. Enaba, A. M. Awadalla. Variability in sphenoid sinus pneumatization and its impact upon reduction of complications following sellar region surgeries. *The Egyptian Journal of Radiology and Nuclear Medicine.* 2014;45(3):705-714.

Table legends

Table 1. Volume values in cm^3 (mean and range) for each of the studied approaches**.**

HS: Hemisphenoidotomy; Max: maximal recorded value; Min: minimal recorded value; PEA: extended transrostral with Posterior Ethmoidectomy Approach; TRA: Transrostral Approach; ETA: Extended Transrostral Approach.

Figure legends

Figure 1. Hemisphenoidotomy (left side). A, lateralization of the middle turbinate; B, visualization of the ostium of the sphenoid sinus; C, enlargement sphenoid sinus ostium; D, view of the posterior wall of the sphenoid sinus.

Mt, middle turbinate; NS, nasal septum; On, optic nerve; psICa, parasellar internal carotid artery; S, sella; So, sphenoid ostium; Ss, intersphenoidal septum; St, superior turbinate.

Figure 2. Transrostral approach (endoscope in right nostril). A, detachment of the sphenoid rostrum; B, removal of the sphenoid rostrum; C, rhomboid-shaped sphenoidotomy; D, rectangular-shaped sphenoidotomy, achieving an adequate opening.

Mt, middle turbinate; NS, nasal septum; R, sphenoid rostrum; S, sella; St, superior turbinate; black dotted line, edges of the sphenoidotomy.

Figure 3. Extended transrostral approach (endoscope in right nostril). A, superior turbinate removal; B, result of right superior turbinectomy; C, enlargement of the sphenoidotomy; D, result of right extended transrostral approach.

Eb, ethmoid bone; Mt, middle turbinate; NS, nasal septum; On, optic nerve; psICa, parasellar internal carotid artery; S, sella; St, superior turbinate.

Figure 4. Extended transrostral with posterior ethmoidectomy approach (endoscope in right nostril). A, curved aspirator showing the additional working space behind the ethmoid bone; B, removal of the posterior part of the ethmoid bone; C, extent of right posterior ethmoidectomy; D, extent of left posterior ethmoidectomy.

Eb, ethmoid bone; Lp, lamina papyracea; Mt, middle turbinate; On, optic nerve; psICa, parasellar internal carotid artery; S, sella.

Figure 5. ApproachViewer screen with all approaches (HS: green; TRA: purple; ETA: light blue; PEA: red) shown in the different planes (A, axial plane; B, coronal plane; C, sagittal plane) and with volume rendering (3D reconstruction). Results of the non-crossing recordings in one specimen are shown.

Figure 6. Recording modalities used during the dissections to quantify the surgical pyramid.

A: Non-crossing modality: the pointer is kept at corresponding positions both at the deep and superficial area (at 12 o'clock in the picture) to record the widest volume that provides the highest surgical maneuverability in bimanual surgery (see text for further details);

B: Crossing modality: the pointer is positioned at opposite points (12 o'clock on deep surface and 6 o'clock at superficial area) so as to record the widest possible deep area.

Figure 7. Surface drawing of the areas of interest. A, visual rendering of the different surfaces at the level of the posterior wall of the sphenoid sinus with an endoscopic view; B, rendering in ApproachViewer of the contoured surfaces.

Sella – half, defined as half of the anterior sellar wall. Bounded medially by the projection of the sphenoidal rostrum, superiorly by the slice tangent to the middle portion of the pituitary gland, inferiorly by the lowest point of the sellar floor, and laterally by the medial wall of the parasellar internal carotid arteries (ICAs).
ICA – Medial half, defined as the surface covering the medial parasellar[1,42] and paraclinoid[43] ICAs. Bounded laterally by the line passing through the cross-sectional centers of the intra- and supra-cavernous ICA, according to Knosp classification,[44] medially by the medial wall of the ICA, superiorly by the sphenoid sinus roof, and inferiorly by the proximal end of the posterior bending of the cavernous ICA.
ICA – Lateral half, defined as the surface covering the lateral parasellar and paraclinoid ICA. Bounded medially by the line passing though the cross-sectional centers of the intra- and supra-cavernous ICA,[44] laterally by the projection of the lateral wall of the ICA, and superiorly and inferiorly as the previous surface.
Inter-ICA distance, defined as the surface between the most medial points of the paraclival ICAs on both sides. Bounded superiorly by the proximal end of the posterior bend of the cavernous ICA, and inferiorly by the sphenoid sinus floor.
Clival recess, defined as the posterior extension of the sphenoid sinus beyond the coronal plane of the pituitary fossa posterior wall.[45,46]
Paraclival ICA, defined as the projection of the paraclival ICA.[1,42,45] Bounded superiorly by the proximal edge of the posterior bend of the cavernous ICA, and inferiorly by the floor of the sphenoid sinus.
VR-line surface, defined as the plane obtained by the 3D conversion of the VR-line,[45] connecting the medial edge of the Vidian canal to the maxillary nerve (V2) in the coronal plane.
Gasserian ganglion, defined as the portion of sphenoid sinus lateral wall not included by the surrounding areas of interest. Bounded anterolaterally by the medial border of the superior orbital fissure.

1, Sella - half; 2, ICA – medial half; 3, ICA – lateral half; 4, inter-ICA distance; 5, Clival recess; 6, Paraclival ICA; 7, Gasserian ganglion; 8, VR-line surface.
LOCR, lateral optico-carotid recess; On, optic nerve; Planum, planum sphenoidale; Sph. Floor, sphenoid sinus floor.

Figure 8. Radar diagrams documenting percentage of exposed areas by each approach, quantified with non-crossing (A) and crossing (B) modalities.

Each circle indicates 20% of additive exposure from 0% (center) to 100% (outer circle).

1, contralateral Sella – half; 2, ipsilateral Sella – half; 3, ipsilateral ICA – medial half; 4, ipsilateral ICA – lateral half; 5, ipsilateral Gasserian ganglion; 6, ipsilateral VR-line surface; 7, ipsilateral Paraclival ICA; 8, inter-ICA distance; 9, Clival recess; 10, contralateral Paraclival ICA; 11, contralateral VR-line surface; 12, contralateral Gasserian ganglion; 13, contralateral ICA – lateral half; 14, contralateral ICA – medial half.

Figure 9. Comparison of approaches. Approaches in rows are compared to the approaches in the columns for each of the areas of interest. Areas of interest are distributed according to the anatomical

subdivision of the posterior wall of the sphenoid sinus. Green cells indicate a statistically significant increase of exposure by performing the approach in the column with respect to the approach in the raw, while red cells indicate a statistically significant loss of exposure.
See text (Results section) for details.

	HS	TRA	ETA	PEA
MEAN	18,57	28,77	35,49	37,20
MIN	10,97	15,82	25,12	27,38
MAX	27,06	41,88	57,66	58,00

Table 1. Volume values (mean and range) for each of the studied approaches.

HS: Hemisphenoidotomy; Max: maximal recorded value; Min: minimal recorded value; PEA: extended transrostral with Posterior Ethmoidectomy Approach; TRA: Transrostral Approach; ETA: Extended Transrostral Approach.

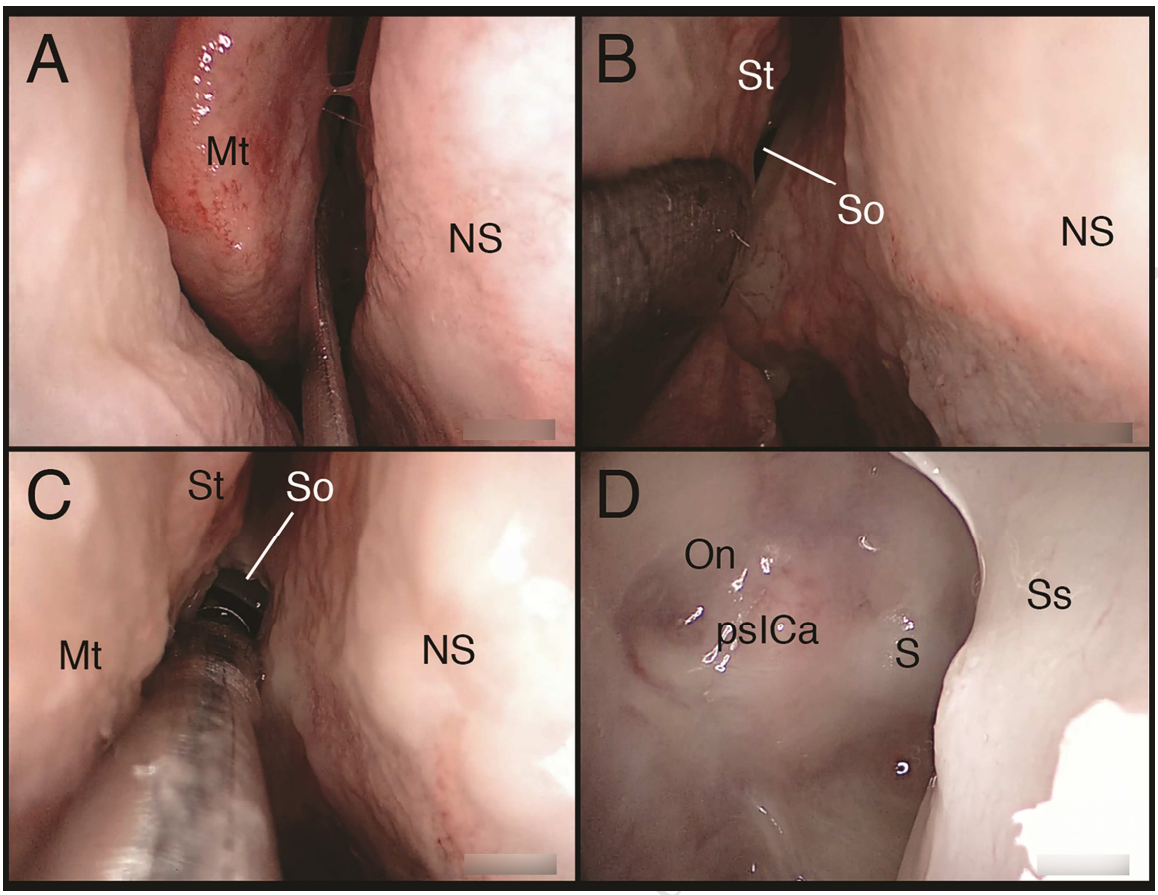

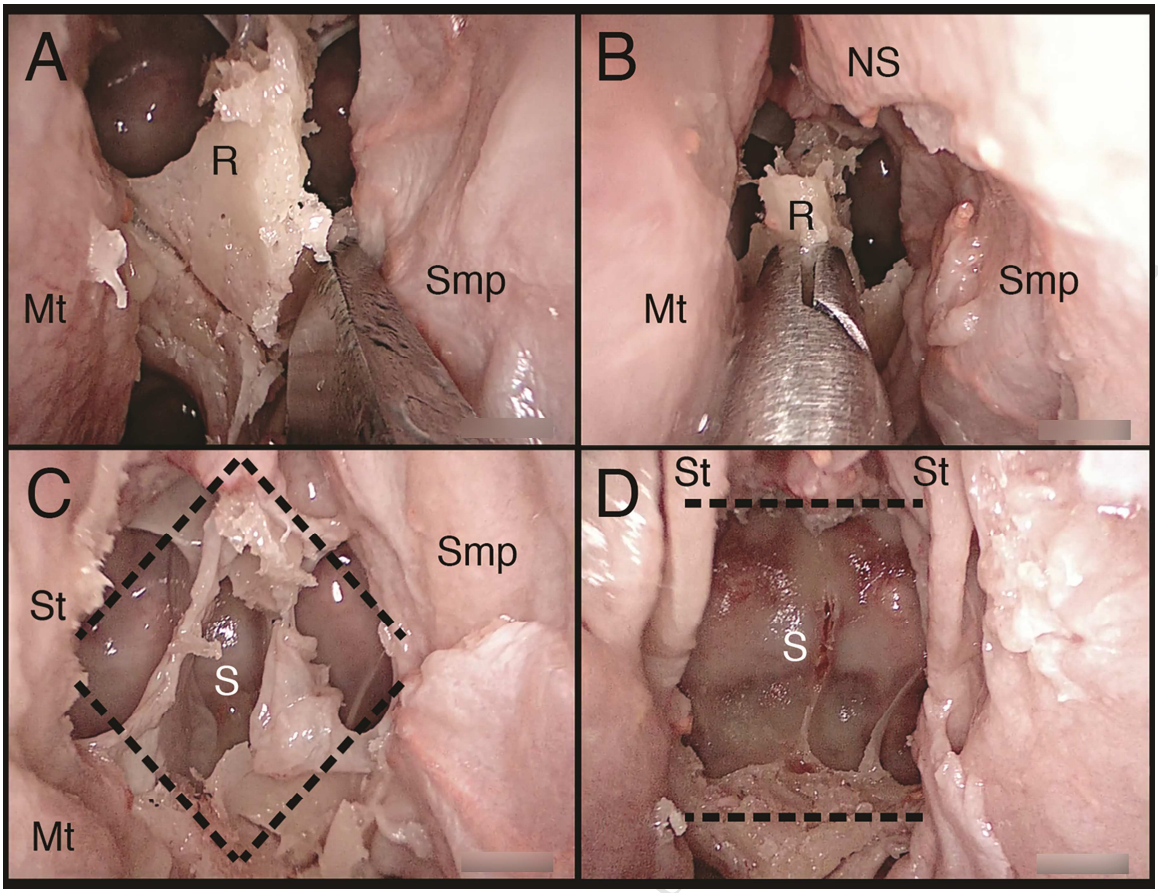

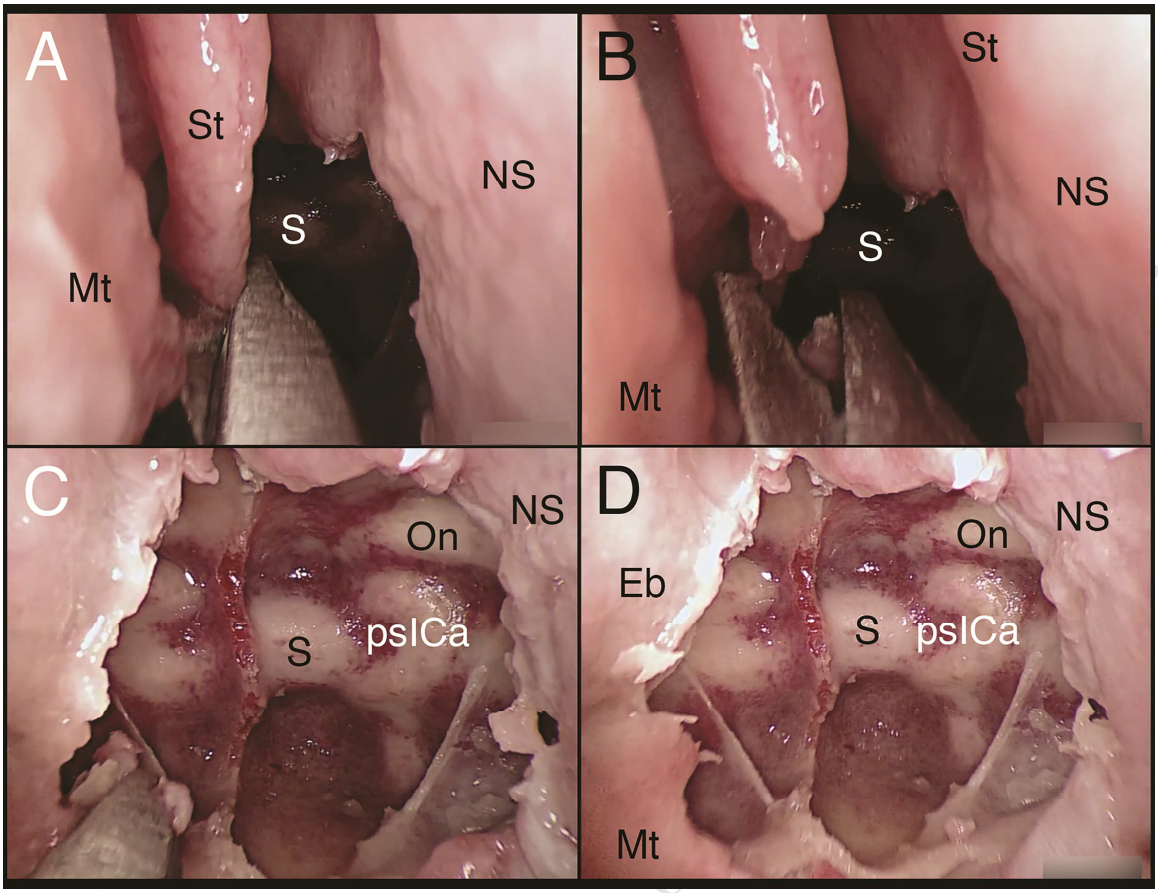

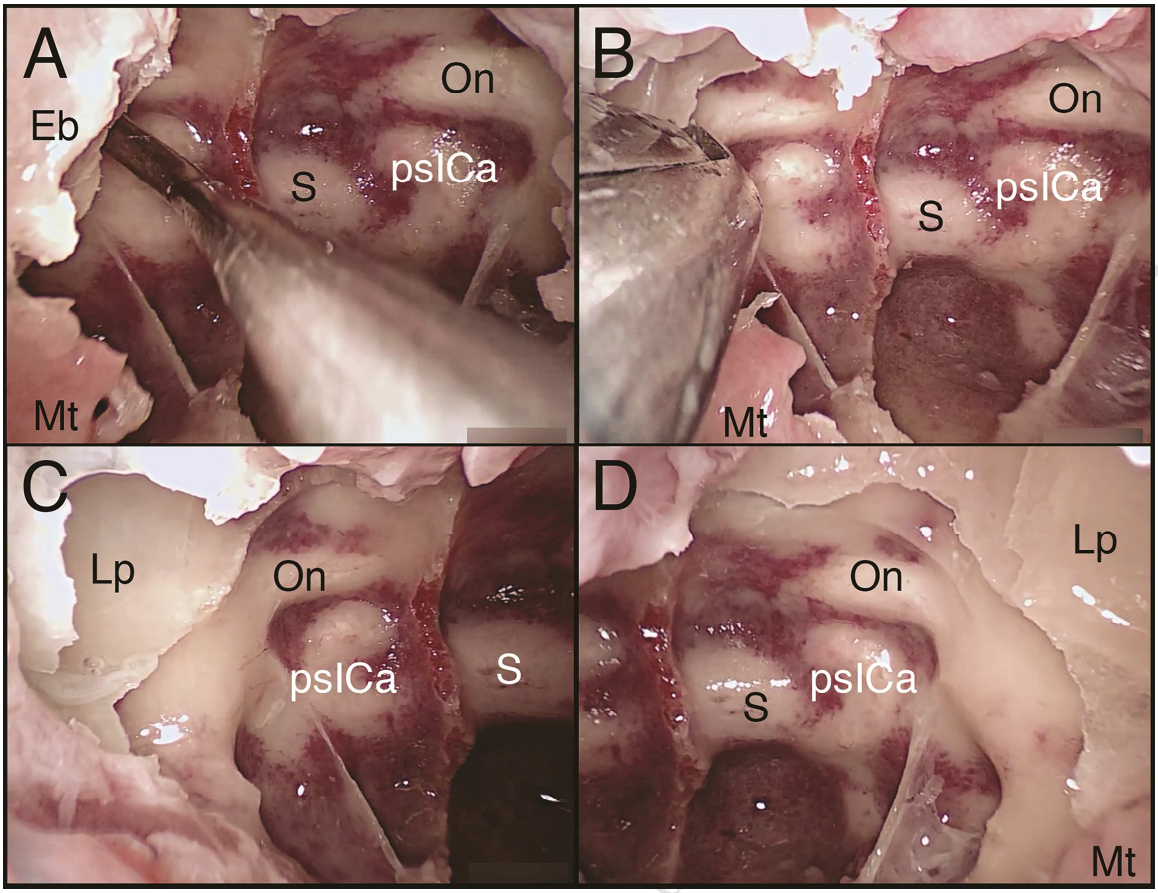

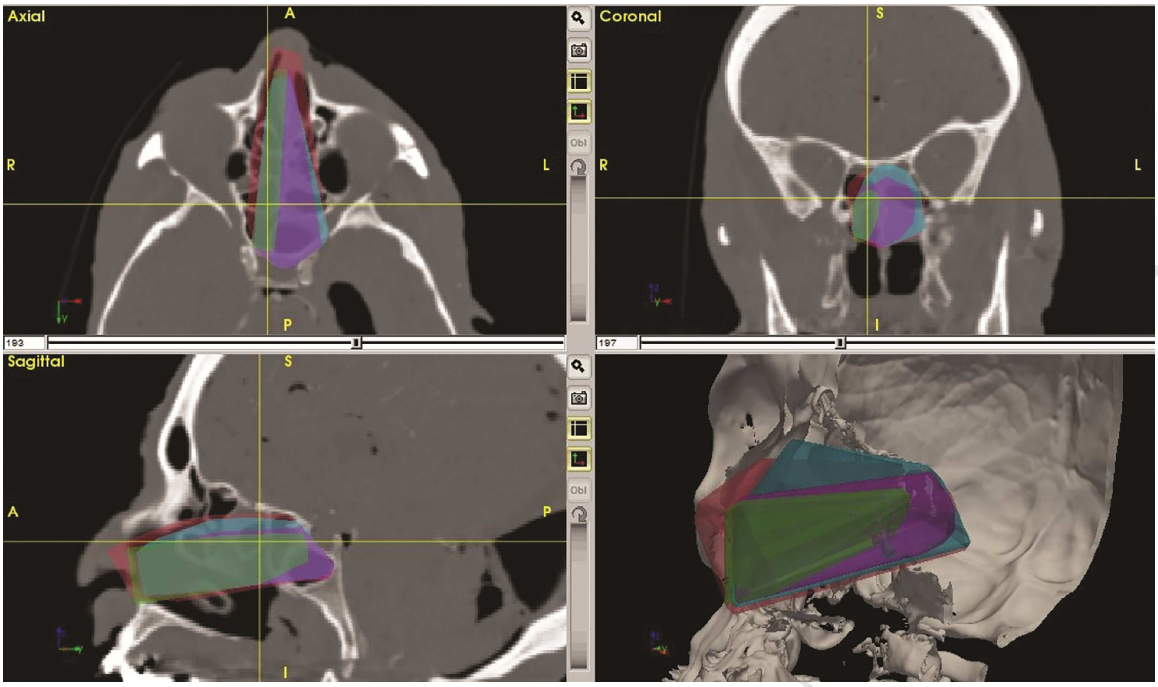

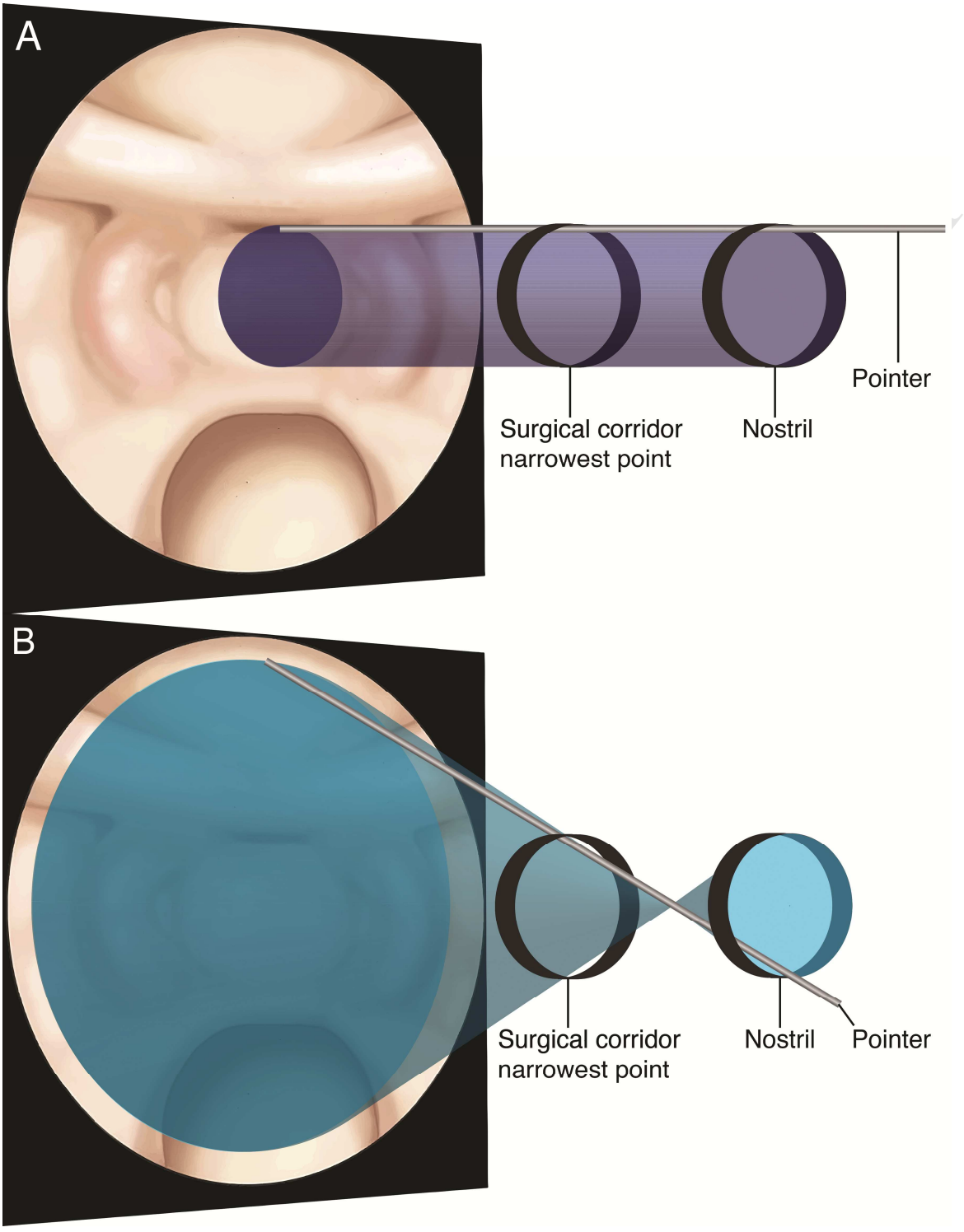
A
Pointer
Surgical corridor
narrowest point
Nostril
B
Surgical corridor
narrowest point
Nostril
Pointer

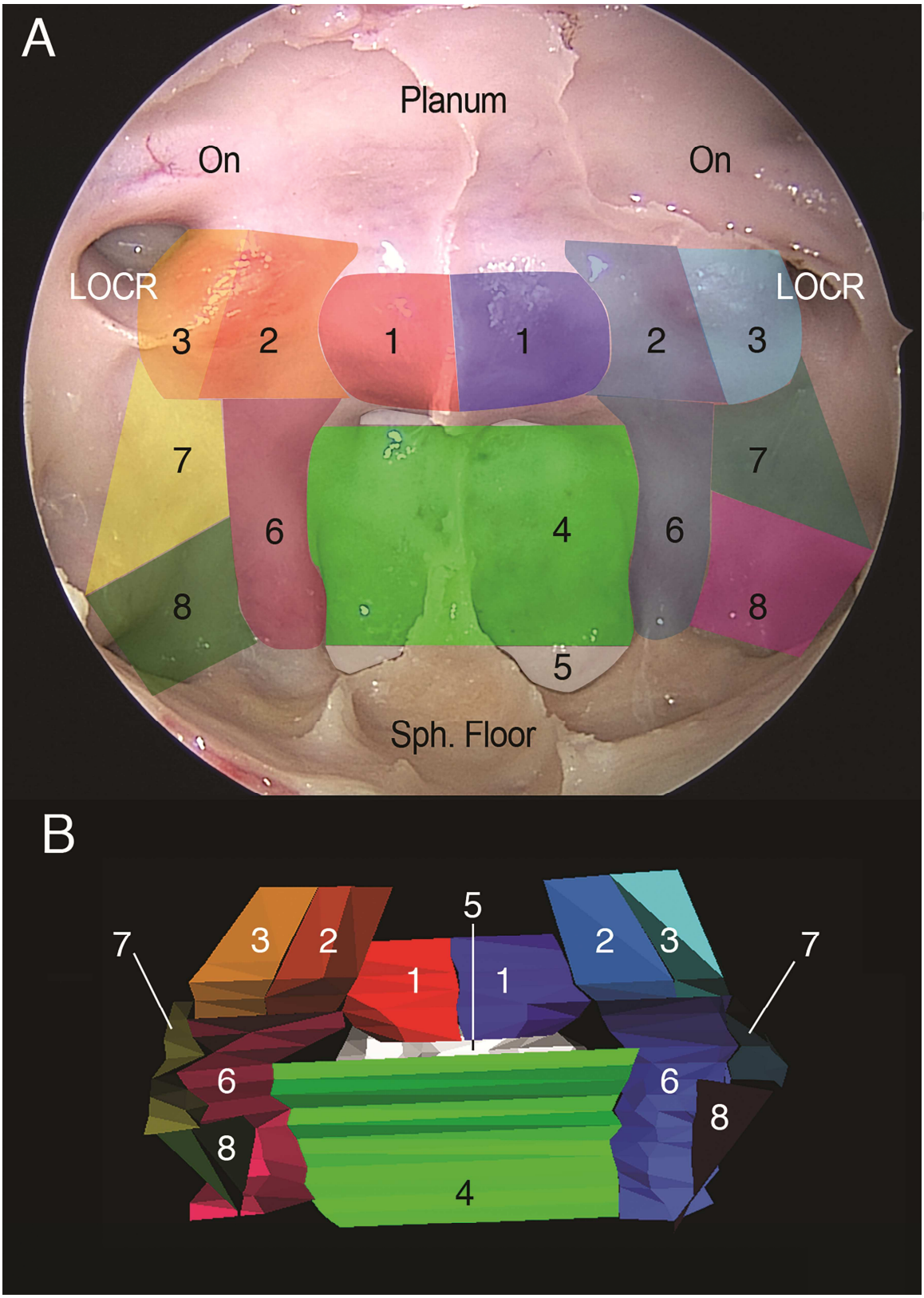
A
Planum
On
On
LOCR
LOCR
3
2
1
1
2
3
7
7
6
4
6
8
8
5
Sph. Floor
B
5
7
3
2
2
3
7
1
1
6
6
8
8
4

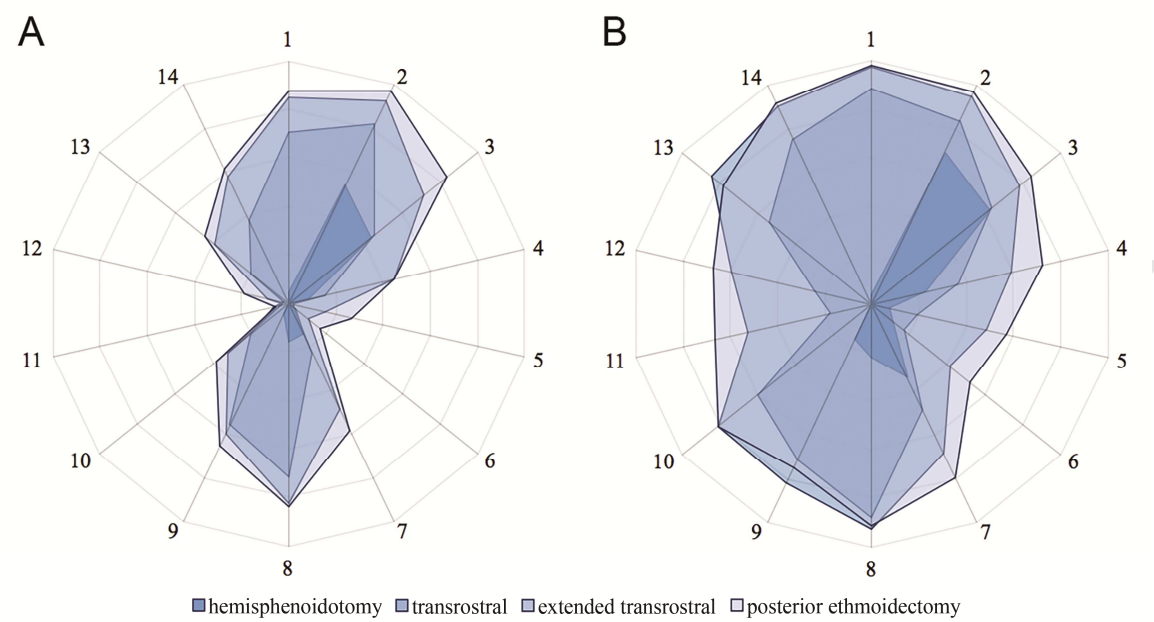

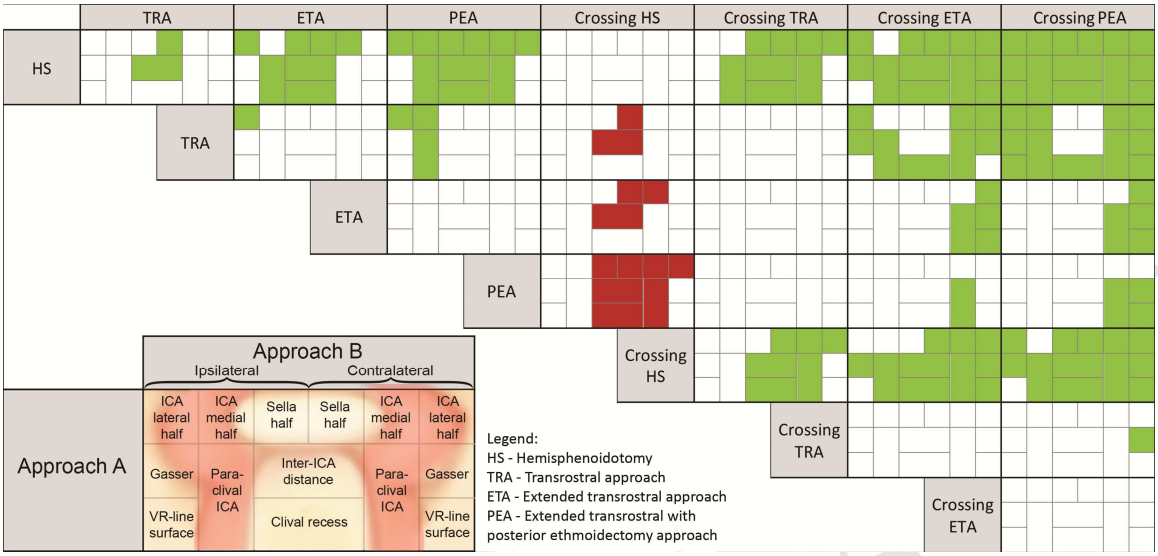

Modular classification of endoscopic endonasal transsphenoidal approaches to the sellar region: anatomical quantitative study

Highlights

1. Multiple variations of the endonasal endoscopic transsphenoidal approach to the sella have been described
2. A modular classification of endoscopic transsphenoidal approaches to the sella is proposed.
3. The intuitive classification is validated by anatomical data with a novel quantification, neuronavigation-based, method.

Modular classification of endoscopic endonasal transsphenoidal approaches to the sellar region: anatomical quantitative study

Francesco Belotti, MD,[1*] Francesco Doglietto, MD, PhD,[1*] Alberto Schreiber, MD,[2] Marco Ravanelli, MD,[3] Marco Ferrari, MD,[2] Davide Lancini, MD,[2] Vittorio Rampinelli, MD,[2] Lena Hirtler, MD,[3] Barbara Buffoli, PhD,[4] Andrea Bolzoni Villaret, MD,[2] Roberto Maroldi, MD,[3&] Luigi Fabrizio Rodella, MD, MSc,[4&] Piero Nicolai, MD,[2&] Marco Maria Fontanella, MD[1&]

Units of [1]Neurosurgery, [2]Otorhinolaryngology and [4]Radiology, Department of Medical and Surgical Specialties, Radiological Sciences and Public Health, University of Brescia, Brescia, Italy
[3]Department of Systematic Anatomy, Center for Anatomy and Cell Biology, Medical University of Vienna
[4]Section of Anatomy and Pathophysiology, Department of Clinical and Experimental Sciences, University of Brescia, Brescia, Italy

All Authors declare they do not have any conflict of interest and do not have anything to disclose.